

A modified phase transfer entropy for cross-frequency directed coupling estimation in brain network

Yalin Wang and Wei Chen, *Senior Member, IEEE*

Abstract—Cross-frequency coupling of neural oscillation is widespread during the complex cognitive process. Therefore, identifying cross-frequency information flow is essential for revealing neural dynamics mechanisms in the brain network. A current method based on the information theory, phase transfer entropy (PTE), has been proved its effectiveness in estimating directional coupling in several recent studies. However, there remains some limits in PTE: (1)lack of multivariable effect, (2) poor robustness, (3)curse of dimensionality in the high dimensional system. This study introduced a novel multivariate phase transfer entropy method named “MPTE_{NUE}” to solve the above issues. In MPTE_{NUE}, it considered the influence of remaining confounding variables, which guaranteed its applicability in a multivariable system. Meanwhile, a nonuniform embedding (NUE) approach for state reconstruction was adopted to eliminate the dimensional curse problem. We performed a series of numerical simulations based on the typical Hénon map model. The results proved that the MPTE_{NUE} achieved better noise robustness and effectively avoided the curse of dimension; meanwhile, the accuracy and sensitivity can reach 96.9% and 99.2%, respectively.

I. INTRODUCTION

As a functionally differentiated complex system, the human brain network shows a typical causal coupling and constitutes a specific directional information flow, which is expected to further illuminate the potential cerebral activity mechanism more accurately and comprehensively. Recent studies have proved that neuronal oscillations of distinct frequencies interact with one another and are associated with functional activities such as communication, computation and thinking[1],[2]. Therefore, quantifying cross-frequency directed coupling is significant in characterising directional couplers between neuronal oscillations and revealing neural dynamics mechanisms in the brain network.

The two most commonly used methods to estimate the directed coupling are Granger causality modelling (GCM) and dynamic causal modelling (DCM). However, these methods faced the following limits: GCM cannot transcribe nonlinear cause-effect relationships without compromising GCM scalability; it may also identify spurious connectivity or even estimate incorrect feedback relations on account of missing relevant information. DCM is a model-driven approach that relies on prior knowledge and needs to consider a dynamic response process to build a better model. As a model-driven approach, it is difficult to build an optimal model. Recently, the phase transfer entropy (PTE) method has attracted wide attention among neuroscientists. When dealing with linear and nonlinear time-series coupling, the PTE has experimentally

proved its superiority in accuracy, robustness, and stability[3]–[5]. However, there remain some limits in PTE. Information flow estimation by PTE required a great deal of data, adjustment of parameters and became vulnerable in the presence of environmental noise, physiological noise. Moreover, the traditional PTE method is a bivariate method; it only evaluates the directed coupling between two isolated phase time-series, while detected neural signals usually include multiple time-series. The causal coupling between any two series is affected by other series; therefore, it is necessary to consider this effect. Another multivariate phase transfer entropy (MPTE) was proposed to extend traditional PTE; regrettably, MTE leads to the “curse of dimensionality”, which will affect the reliability of directed information flow[6], [7].

In this study, a modified PTE method named “MPTE_{NUE}” was proposed to make it more suitable for analysing neurophysiological signals. We extended the traditional bivariate PTE by considering the effects of remaining confounding variables when calculating the causal relationship between the two variables. Moreover, we adopted the nonuniform embedding (NUE) method to solve the curse of dimension[8]. We carried out a series of numerical simulations to verify the performances of MPTE_{NUE} and compared them with the traditional PTE. This paper is structured as follows. The theory of the proposed method is detailed in Section II. The numerical simulation results are provided in Section III. The discussion and conclusion are summarised in Section IV.

II. PROPOSED METHOD

A. Related phase transfer entropy

The phase transfer entropy (PTE) for neurophysiological signal analysis was first proposed by Lobier et. al. in 2014[5]. It is a typical bivariate causality estimation based on the following principle: suppose there are two sequences, namely driving sequence $X(t)$ and target sequence $Y(t)$ respectively, if $X(t)$ has a causal effect on $Y(t)$, the uncertainty of the present of $Y(t)$ conditioned on its own past $Y(t - \delta)$ should be greater than the uncertainty of the present of $Y(t)$ conditioned on the signals of both past $X(t - \delta)$ and $Y(t - \delta)$. In this PTE algorithm, the Shannon entropy was adopted to measure the uncertainty of the sequence $X(t)$. Firstly, for a series $X(t)$ in a given frequency band, its phase time-series $\theta(t)$ can be obtained by Hilbert transform:

$$X(t) = A(t)e^{i\theta(t)} \quad (1)$$

This work is supported by Shanghai Municipal Science and Technology Major Project (Grant No. 2017SHZDZX01).

Yalin Wang and Wei Chen are with the School of Information Science and Technology, Fudan University, Shanghai 200433, China, and also with the Human Phenome Institute, Fudan University, Shanghai 201203, China.

*Corresponding Authors: Wei Chen: w_chen@fudan.edu.cn.

where $A(t)$ is the instantaneous amplitude of $X(t)$. For $X(t)$ and $Y(t)$, the corresponding phase time-series are $\theta_X(t)$ and $\theta_Y(t)$, so the PTE from $X(t)$ to $Y(t)$ is defined as:

$$\text{PTE}_{X \rightarrow Y} = H(\theta_Y(t), \theta_Y(t - \delta)) + H(\theta_Y(t - \delta), \theta_X(t - \delta)) - H(\theta_Y(t - \delta)) - H(\theta_Y(t), \theta_Y(t - \delta), \theta_X(t - \delta)) \quad (2)$$

where $H(\cdot)$ is marginal Shannon entropy:

$$H(X) = -\sum_{x \in X} p(x) \log(p(x)) \quad H(X, Y) \text{ is the joint Shannon entropy, } H(X, Y) = -\sum p(x, y) \log(p(x, y)). \text{ And } p(\cdot) \text{ is the probability description.}$$

B. Multivariate phase transfer entropy based on NUE

Based on the traditional PTE, we establish multivariate phase transfer entropy (MPTE). In this study, we consider a multivariate dataset $\{X, Y, Z_1, Z_2, \dots, Z_{N-2}\}$, where X is driving series, Y is target series, and $Z = \{Z_2, \dots, Z_{N-2}\}$ are the remaining confounding series. We get their phase time-series $\{\theta^X, \theta^Y, \theta^Z\}$ through the Hilbert transform. The estimation of MPTE also involves the formulation of uniformly spaced embedding vectors from each variable. For phase time-series θ^X , the corresponding embedding vector is defined as:

$$\theta_t^X = [\theta_t^X, \theta_{t-\delta}^X, \dots, \theta_{t-(m-1)\delta}^X] \quad (3)$$

where m is the embedding dimension and δ is the time lag.

MPTE from X to Y conditioning on Z can be defined as:

$$\text{MPTE}_{X \rightarrow Y|Z} = I(\theta_{t+1}^Y; \theta_t^X | \theta_t^Y, \theta_t^Z) = H(\theta_t^X, \theta_t^Y, \theta_t^Z) + H(\theta_{t+1}^Y, \theta_t^Y, \theta_t^Z) - H(\theta_{t+1}^Y, \theta_t^X, \theta_t^Y, \theta_t^Z) - H(\theta_t^Y, \theta_t^Z) \quad (4)$$

where $I(\cdot | \cdot)$ defines the conditional mutual information (CMI) and $H(\cdot)$ is the joint Shannon entropy. For a series θ^X , Shannon entropy is defined as:

$$H(\theta^X) = -\sum p(\theta^X) \log(\theta^X) \quad (5)$$

where $p(\theta^X)$ is the probability mass function of the outcome θ^X , typically estimated by the relative frequency of θ^X . Entropy estimation in Eq. (4-5) can be realised based on random variable discretisation by calculating the probability densities. Here, we use the k -nearest neighbours (KNN) estimator because of its best effectiveness for high-dimensional data, and the number of neighbours is set as 10[9]. For each reference point, viewed in the largest state-space, the distance length is defined as the distance to the K^{th} nearest neighbour. Then, densities at projected subspaces are locally formed by the number of points within ϵ from each reference point.

Further, we introduced a new embedding strategy, nonuniform embedding (NUE) into the MPTE. We formed a set of variables to represent the past state of the time series. We set the maximum of time delay for phase time-series, δ_X for θ^X and δ_Y for θ^Y and δ_Z for θ^Z , and the delays of θ^X, θ^Y , and θ^Z are sought within a range of 1~ maximum for each variable. W_t is defined as the set of all lagged variables at time t , containing the parts $\theta_t^X, \theta_{t-1}^X, \theta_{t-2}^X, \dots, \theta_{t-\delta_X}^X$ of phase time-series θ^X and the same for θ^Y and θ^Z . We use an iterative scheme to generate the NUE vector. Firstly, we initialise an empty embedding vector $W_n^0 = \emptyset$. And then, we start an iteration processing. In the first iteration, $k=1$, we find the component in W_t^1 being most correlated to θ^Y given by the KNN estimator of mutual information. At the same time, W_t^1 is removed from W_t

$$W_t^1 = \arg \max I(\theta^Y; W_t) \quad (6)$$

where $I(\cdot)$ is the mutual information. In the middle iteration, $k>1$, the mixed embedding vector is augmented by the component W_t^k of W_t , giving most information about y_t additionally to the information already contained in the $W_t^{k-1} = [W_t^1, W_t^2, \dots, W_t^{k-1}]$, W_t^{k-1} will be selected by a standard through calculating the maximum value of the conditional mutual information:

$$W_t^k = \arg \max I(\theta^Y; W_t | V_t^{k-1}) \quad (7)$$

where conditional mutual information $I(\cdot)$ is again estimated by the KNN. By using the greedy forward method, each W_t^k will be embedded in the already embedded vector V_t^{k-1} until the process stops. The termination criterion is quantified as:

$$\frac{I(\theta^Y; V_t^{k-1})}{I(\theta^Y; V_t^k)} > T \quad (8)$$

Referring to the previous study, in our work, we set the threshold T as 0.95[10]. So that, this embedding process stop and an NUE vector $V_t = V_t^{k-1}$ is obtained. Any combination of the lagged variables $\theta^X, \theta^Y, \theta^Z$ maybe included in V_t .

To quantify the causal effect of θ^X on θ^Y conditioned by the remaining confounding series θ^Z , we calculated a novel MPTE_{NUE} by:

$$\text{MPTE}_{\text{NUE}}(X \rightarrow Y|Z) = \frac{I(\theta^Y; V_t^X | V_t^Y, V_t^Z)}{I(\theta^Y; V_t)} \quad (9)$$

where V_t^X represents the component of θ^X in V_t . It is the same with V_t^Y and V_t^Z . Neurophysiological signals such as EEG are usually multi-channel signals covering the corresponding regions of interest (ROIs). It usually involves directional information flow between ROIs, not only channels. Here we extend the MPTE_{NUE} method to solve this limit.

Suppose that ROI “ M ” contains m channels series, $(x_1(t), x_2(t), \dots, x_m(t))$, ROI “ N ” contains n channels series $(y_1(t), y_2(t), \dots, y_n(t))$, then the information flow from ROI M to ROI N is calculated as follows:

$$\text{MPTE}_{\text{NUE}}(M \rightarrow N) = \frac{1}{MN} \sum_{m=1}^M \sum_{n=1}^N \text{MPTE}_{\text{NUE}}(X_m \rightarrow Y_n | Z) \quad (10)$$

In this study, EEGlab toolbox was used to preprocess the acquired EEG signal. The EEG data was filtered with a bandpass of 1~40Hz using the finite impulse response (FIR) filter to eliminate the noise. Then independent component analysis (ICA) was applied to eliminate EOG artifacts. Subsequently, we calculated the corresponding phase time-series in the specific frequency band (namely, $\alpha, \beta, \delta, \theta$) by the Hilbert transform, and finally estimated the causal coupling using the proposed MPTE_{NUE} method. The flow chart of directional coupling estimation is shown in Fig.1.

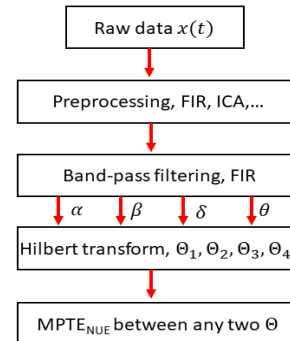


Fig.1. Schematic diagram of cross-frequency directed coupling algorithms.

Neurophysiological signals generate a typical high-dimensional system, and it brings about the curse of dimension in traditional methods, which leads to lower accuracy in causal estimation. Here we define “*Acc*”, and “*Sen*” as the quantitative indicators for accuracy and sensitivity separately in causality assessment methods[11]:

$$Acc = \frac{TP+TN}{TP+TN+FN+FP} \quad (11)$$

$$Sen = \frac{TP}{TP+FN} \quad (12)$$

where *TP* is true positive, *TN* means true negative, *FN* stands for false negative, and *FP* is false positive.

III. NUMERICAL SIMULATION RESULTS

The Hénon map is a multidimensional dynamical system with discrete time series, which is proposed firstly by Michel Hénon[12]; the model coupling diagram is shown in Fig.2. As a common nonlinear, non-stationary causal system, coupled Hénon map model is widely used in numerical simulation analysis[13], [14]. In this study, the Hénon map model for phase series with *M* variates was generated according to the following formula:

$$S_m(n) = \sin(2\pi \cdot 1000n) \cdot e^{iX_m(n)}, m \in [1, 2, \dots, M] \quad (13)$$

where $X_m(n)$ can be modified as follows:

$$X_i(n) = 1.4 - X_i^2(n-1) + 0.3X_i(n-2), i = 1, M. \quad (14)$$

$$X_j(n) = 1.4 - \left(0.5C \left(X_{j-1}(n-\delta) + X_{j+1}(n-\delta)\right) + (1 - C)X_j(n-1)\right)^2 + 0.3X_j(n-2), j = 2, 3, \dots, M-1. \quad (15)$$

where $n = 1, 2, \dots, L$, L is the length of time series. The parameter C was varied to modulate the coupling strength from the $(i+1)^{\text{th}}$ and the $(i-1)^{\text{th}}$ systems towards the i^{th} system, δ defines the coupling delay between two variates; in this study, we set $\delta = 3$. This simulated data satisfies the non-stationarity and nonlinearity of neurophysiological signals.

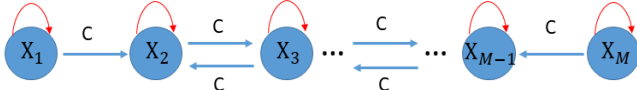


Fig.2. The coupling diagram of the Hénon map model

We verified the performance of the proposed $MPTE_{NUE}$ method by a series of numerical simulations. The simulation data is set as a 4-variable Hénon map model, and the simulation aspect mainly included data length L , coupling strength C , and signal-to-noise ratio (SNR). Firstly, we compared the robustness of our $MPTE_{NUE}$ with traditional PTE, MPTE method for the data length L . We established the Hénon map model, where C was 0.5, and the data length increased from 500 to 6000, with the step of 250. The transfer entropy results are shown in Fig.3. Compared with the other two methods, it is evident that our $MPTE_{NUE}$ method realises better stability in the whole range. Even when the data length is small, $MPTE_{NUE}$ can estimate higher causal strength results. Therefore, our method is more robust to the data length.

We also investigated the relationship between the model coupling parameter “ C ” and the calculated causal strength. As shown in Fig.4, we can see that the causal strength obtained by the proposed $MPTE_{NUE}$ method is higher than that obtained by the traditional methods, MPTE and PTE. The causal strength results obtained by $MPTE_{NUE}$ are positively

correlated with C in the whole range from 0.1 to 0.9, while other methods have poor effects and cannot always positively correlate with C . For example, the causality strength $X_1 \rightarrow X_2$, $X_4 \rightarrow X_3$ calculated by the PTE method does not increase with the increase of “ C ”.

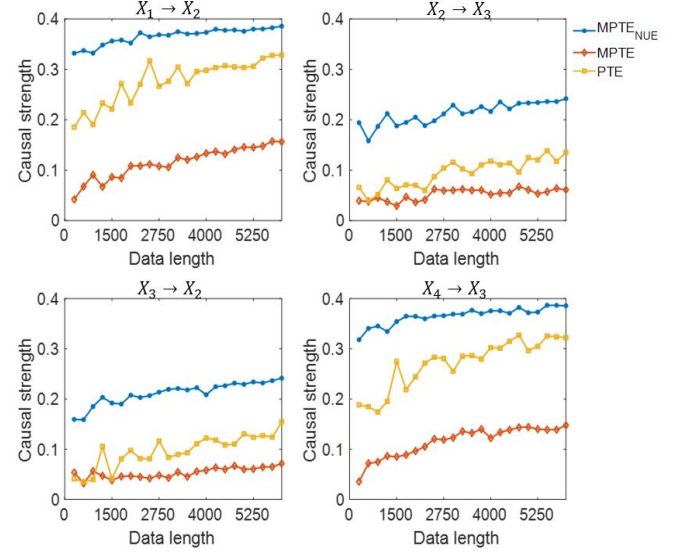


Fig.3. The causal strength of the Hénon map model was calculated by $MPTE_{NUE}$, MPTE and PTE methods on different data lengths L with the coupling coefficient $C=0.5$.

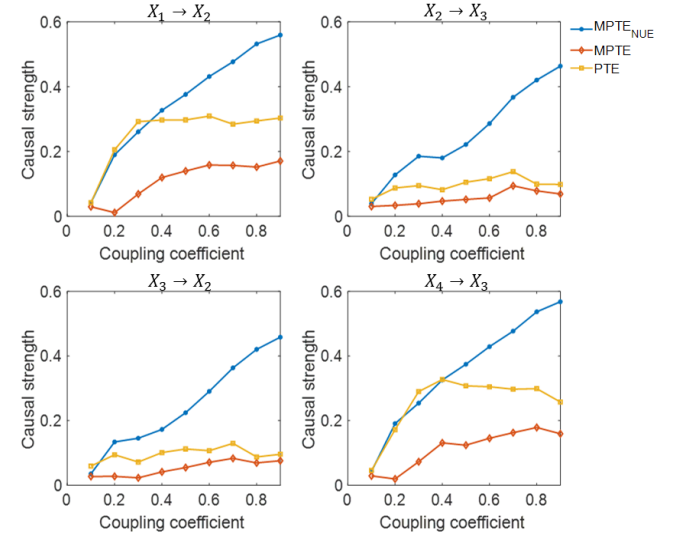


Fig.4. The causal strength of the Hénon map model was calculated by $MPTE_{NUE}$, MPTE, and PTE methods on different coupling coefficients C with the data length $L=4000$.

We also consider the noise interference condition to study the effect of causal estimation. Similarly, we use the Hénon map model, where C is 0.5, and the data length L is 4000. The white Gaussian noise is added to the original series, and the SNR conditions are set from 10dB to 50dB, with a step of 2dB. The result is shown in Fig. 5. $MPTE_{NUE}$ results maintained better stability in the whole SNR range, and under the strong noise condition (namely low SNR), $MPTE_{NUE}$ still estimated the significant strong causal coupling. So that $MPTE_{NUE}$ demonstrates superior noise robustness.

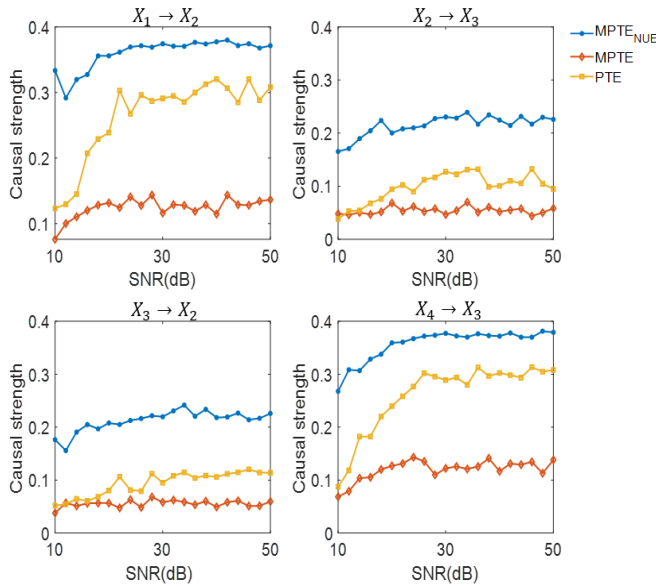


Fig. 5. The causal strength of the Hénon map model was calculated by MPTE_{NUE}, MPTE and PTE methods on different SNR with $L=4000$, $C=0.5$.

We also studied the accuracy and sensitivity of causal estimation in the high-dimensional system with SNR=20dB, length $L=4000$. Here, we considered 100 realisations for each Hénon map causal coupling with the model dimensionality $M=30$. The results of accuracy and sensitivity are shown in Tab.I. Compared with the other two methods, it is obvious that our MPTE_{NUE} method achieves the highest accuracy and sensitivity, 96.9% and 99.2%, respectively.

Tab.I. The *Acc* and *Sen* results of three methods

	MPTE _{NUE}	MPTE	PTE
<i>Acc</i>	96.9%	73.6%	85.8%
<i>Sen</i>	99.2%	79.9%	84.4%

IV. DISCUSSION AND CONCLUSION

This study proposed a novel directed coupling method, MPTE_{NUE}, for brain network evaluation and verified its effectiveness and superiority. Of course, the study remains a few limitations. We only adopted the classical Hénon map model in the numerical verification, considering the data length, SNR, and coupling parameters C . In addition to the Hénon map model, the widely used coupling system models include linear auto-regressive (AR) model, auto-regressive fractionally integrated moving average (ARFIMA) process, Rössler system model, neural mass model and so on[14]–[16]. Future studies will consider the simulation above these models to further validate the performances of the proposed method. In future studies, more numerical models mentioned above will be used for performance verification. At the same time, the MPTE_{NUE} method will also be applied to neurophysiological signals, such as EEG, to explore more brain science questions.

To conclude this study, based on the traditional PTE and nonuniform embedding methods, a novel MPTE_{NUE} method of directional information flow was proposed in this paper. It considered the influence of remaining confounding variables. Meanwhile, it improved the robustness and solved the curse of dimension successfully. The results proved the superiority of

the proposed MPTE_{NUE} method, with the accuracy and sensitivity reaching 96.9% and 99.2%, respectively.

REFERENCES

- [1] O. Jensen and L. L. Colgin, "Cross-frequency coupling between neuronal oscillations," *Trends in Cognitive Sciences*, vol. 11, no. 7, pp. 267–269, 2007, doi: 10.1016/j.tics.2007.05.003.
- [2] S. Dimitriadis, Y. Sun, N. Laskaris, N. Thakor, and A. Bezerianos, "Revealing Cross-Frequency Causal Interactions During a Mental Arithmetic Task Through Symbolic Transfer Entropy: A Novel Vector-Quantization Approach," *IEEE Transactions on Neural Systems and Rehabilitation Engineering*, vol. 24, no. 10, pp. 1017–1028, Oct. 2016, doi: 10.1109/TNSRE.2016.2516107.
- [3] R. Wang, S. Ge, N. M. Zommará, K. Ravienna, T. Espinoza, and K. Iramina, "Consistency and dynamical changes of directional information flow in different brain states: A comparison of working memory and resting-state using EEG," *NeuroImage*, vol. 203, p. 116188, 2019, doi: 10.1016/j.neuroimage.2019.116188.
- [4] Y. Wang and W. Chen, "Effective brain connectivity for fNIRS data analysis based on multi-delays symbolic phase transfer entropy," *Journal of Neural Engineering*, vol. 17, no. 5, p. 056024, 2020, doi: 10.1088/1741-2552/abb4a4.
- [5] M. Lobier, F. Siebenhühner, S. Palva, and J. M. Palva, "Phase transfer entropy: A novel phase-based measure for directed connectivity in networks coupled by oscillatory interactions," *NeuroImage*, vol. 85, pp. 853–872, 2014, doi: 10.1016/j.neuroimage.2013.08.056.
- [6] J. Runge, "Causal network reconstruction from time series: From theoretical assumptions to practical estimation," *Chaos*, vol. 28, no. 7, p. 075310, 2018, doi: 10.1063/1.5025050.
- [7] J. Runge, J. Heitzig, V. Petoukhov, and J. Kurths, "Escaping the curse of dimensionality in estimating multivariate transfer entropy," *Phys Rev Lett*, vol. 108, no. 25, p. 258701, Jun. 2012, doi: 10.1103/PhysRevLett.108.258701.
- [8] D. Kugiumtzis, "Direct-coupling information measure from nonuniform embedding," *Phys Rev E Stat Nonlin Soft Matter Phys*, vol. 87, no. 6, p. 062918, Jun. 2013, doi: 10.1103/PhysRevE.87.062918.
- [9] A. Kraskov, H. Stögbauer, and P. Grassberger, "Estimating mutual information," *Phys Rev E Stat Nonlin Soft Matter Phys*, vol. 69, no. 6 Pt 2, p. 066138, Jun. 2004, doi: 10.1103/PhysRevE.69.066138.
- [10] I. Vlachos and D. Kugiumtzis, "Nonuniform state-space reconstruction and coupling detection," *Phys Rev E Stat Nonlin Soft Matter Phys*, vol. 82, no. 1 Pt 2, p. 016207, 2010, doi: 10.1103/physreve.82.016207.
- [11] J. Niu, Y. Tang, Z. Sun, and W. Zhang, "Inter-Patient ECG Classification With Symbolic Representations and Multi-Perspective Convolutional Neural Networks," *IEEE Journal of Biomedical and Health Informatics*, vol. 24, no. 5, pp. 1321–1332, May 2020, doi: 10.1109/JBHI.2019.2942938.
- [12] M. Hénon, "A two-dimensional mapping with a strange attractor," *Communications in Mathematical Physics*, vol. 50, no. 1, pp. 69–77, 1976, doi: 10.1007/BF01608556.
- [13] A. Krakovská, J. Jakubík, M. Chvosteková, D. Coufal, N. Jajcay, and M. Paluš, "Comparison of six methods for the detection of causality in a bivariate time series," *Physical review. E*, vol. 97, no. 4–1, p. 042207, Apr. 2018, doi: 10.1103/physreve.97.042207.
- [14] X. Mao and P. Shang, "Transfer entropy between multivariate time series," *Communications in Nonlinear Science and Numerical Simulation*, vol. 47, pp. 338–347, 2017, doi: 10.1016/j.cnsns.2016.12.008.
- [15] P. Yang, P. Shang, and A. Lin, "Financial time series analysis based on effective phase transfer entropy," *Physica A: Statistical Mechanics and its Applications*, vol. 468, pp. 398–408, 2017, doi: 10.1016/j.physa.2016.10.085.
- [16] J. Liu, G. Tan, Y. Sheng, and H. Liu, "Multiscale transfer spectral entropy for quantifying corticomuscular interaction," *IEEE Journal of Biomedical and Health Informatics*, pp. 1–1, 2020, doi: 10.1109/JBHI.2020.3032979.